



HAL
open science

Mechanical Behavior of Flax Fibers during Cyclic Tensile Tests in a Controlled Humid Environment

Erwan Huguet, Stéphane Corn, Nicolas Le Moigne, Patrick Ienny

► **To cite this version:**

Erwan Huguet, Stéphane Corn, Nicolas Le Moigne, Patrick Ienny. Mechanical Behavior of Flax Fibers during Cyclic Tensile Tests in a Controlled Humid Environment. ICCM 23 - 23rd International Conference on Composites Materials, Queen's University Belfast, Jul 2023, Belfast, United Kingdom. hal-04193141

HAL Id: hal-04193141

<https://hal.science/hal-04193141>

Submitted on 4 Dec 2023

HAL is a multi-disciplinary open access archive for the deposit and dissemination of scientific research documents, whether they are published or not. The documents may come from teaching and research institutions in France or abroad, or from public or private research centers.

L'archive ouverte pluridisciplinaire **HAL**, est destinée au dépôt et à la diffusion de documents scientifiques de niveau recherche, publiés ou non, émanant des établissements d'enseignement et de recherche français ou étrangers, des laboratoires publics ou privés.

MECHANICAL BEHAVIOR OF FLAX FIBER BUNDLES DURING CYCLIC TENSILE TESTS IN A CONTROLLED HUMID ENVIRONMENT

E. Huguet¹, S. Corn¹, N. Le Moigne² and P. Jenny¹

¹ LMGC, Univ Montpellier, IMT Mines Ales, CNRS, Ales, France, erwan.huguet@mines-ales.fr, stephane.corn@mines-ales.fr, patrick.jenny@mines-ales.fr

² Polymères Composites et hybrides (PCH), IMT mines Ales, Ales, France, nicolas.le-moigne@mines-ales.fr

Keywords: flax fiber, hygro-mechanical behavior, loading-unloading, tensile test

ABSTRACT

The mechanical response of plant fibers to tensile loading is non-linear and related to their moisture content. In order to model this complex behavior, it is necessary to evaluate it at different strain rates. In this study, flax fiber bundles are subjected to cyclic loading and unloading tensile tests. Tensile tests were performed at three crosshead speeds (0.1 mm/min, 1 mm/min, 10 mm/min). Moreover, the samples were tested in different relative humidity conditions (15%, 50%, 75%). On the one hand, the results show that flax bundles exhibited a non-linear mechanical behavior in the first tensile cycle with significant residual strain. During the following tensile cycles, the stress-strain curve tends to become linear with less residual strain. Moreover, all these stress-strain curves become almost superimposed between the fourth and tenth tensile cycle. Finally, the impact of the tensile speed and the relative humidity is investigated via the comparison of mechanical properties such as the maximum tangent elastic modulus, the residual strain after each cycle and the area of the stress-strain hysteresis. The influence of these different testing conditions on the visco-elasto-plastic behavior of flax fiber bundles is then discussed to develop a predictive mechanical model.

1 INTRODUCTION

The use and interest of industries for bio-composite materials using plant fibers as reinforcement is growing. The study of the mechanical behavior of plant fibers is an important turning point for innovation. Comprehensive information on mechanical tensile characteristics of plant fibers can be found in references [1], [2]. On the other hand, the complex mechanical behavior of plant fibers with non-linear stress-strain curves has been revealed [3]. In the last years, the most comprehensive analyses were mostly conducted on flax and hemp elementary fibers [2], [4]. To describe this behavior, the stress-strain curves have been classified into three different types. Type I: Linear strain-stress curve, Type II: linear with a decrease in stiffness from a threshold Type III: Linear at the beginning of the strain-stress curve then followed by a non-linear part during which the stiffness decreases then increases. Several hypotheses have been proposed to explain the non-linearity of stress-strain curves for plant fibers: (1) the modification of the micro-fibrillar angle (MFA) during a mechanical test [5], [6] (2) the presence of defects and dislocation zones within the ultrastructure of elementary fibers [7], [8] (3) the crystallization of a part of the amorphous cellulose in the cell walls during the mechanical test [9] and (4) the non-linearity of the compliance of the tensile system including the force cell and the link between the sample and the jaws of the traction machine (most of the time a glue or a resin) [10].

In order to investigate these different hypotheses, it is essential to analyze the different events occurring during a tensile test in well-controlled testing conditions. It is thus interesting to subject plant fibers to cyclic tensile tests, which has been done on hemp elementary fibers [11] and flax bundles [12]. These works showed the occurrence of residual deformation and stiffening of the samples after each load-unload tensile cycle. These observations led to the development of a micro-mechanical model, aiming to describe this complex mechanical behavior [13]. However, in order to enrich this type of model, it is important to perform these experimental analyses with different cyclic test parameters.

Besides, the visco-elastic behavior of some plant fibers has been studied by creep test, or by nano-indentation [14]–[16]. This work has shown that the time dependency of the mechanical behavior has to be considered with the influence of the moisture content in the fiber cell walls. Indeed, it has been shown that moisture content has a major impact on the morphology [17], tensile properties [18] and visco-elastic behavior [13] of plant fibers. These observations are similar to those made on wood fibres [19]. The use of plant fiber can therefore impact on the viscous behavior of a bio-composite material. This is why the study of the visco-elastic behavior of plant fibers is necessary to develop biocomposites materials. Therefore, the aim of this study is to study the impact of tensile speed and relative humidity (RH) on the mechanical behavior of plant fibers during cyclic tensile tests. Experiments were carried out on flax fiber bundles in controlled humid conditions from 15 %RH to 75 %RH. The influence of the tensile speed was also studied from 0.1mm/min to 10mm/min to analyze their visco-elastic behavior.

2 EXPERIMENTAL METHOD

2.1 Material

The flax fiber bundles used were extracted from a *linium usitatissimum* (Alizee, Grandvilliers, France, 2012) batch. Other previous works have been done on the same batch of fibers with similar extraction methods [17], [20], [21]. For each combination of tensile speed and RH, 15 samples were tested. Fibers that were broken during the cyclic tensile test (5 trials out of 135 in total) were excluded from data analysis. Before all test, each bundle is glued at each end to a plastic tab using a photo-curing glue (DYMAX, Wiesbaden, Germany). This method is further described in previous works [21].

2.2 Fibers conditioning and environmental conditions

The morphological measurements and mechanical tests were carried out at 23°C and 15, 50 and 75 %RH in a controlled environment chamber (ETS model 5532 chamber, ETS electro-tech systems, Perkasi Pennsylvania, USA). Samples were before conditioned at the corresponding RH and temperature for 12 hours.

2.3 Morphological measurements

All morphological analyses were carried using FDAS apparatus (Diastron Ltd, Hampshire, UK). Considering a filtered elliptical model, as described in previous works [21], the median cross section area (CSA) of each fiber bundle was calculated from the apparent diameters measured at controlled RH before and after mechanical tests.

In this work, each bundle underwent a FDAS measurement to estimate its median elliptic CSA before and after the tensile test. The results of these measurements are presented in Figure 1 concerning the CSA. At first it is important to underline the great variability of elliptical CSA value of the samples. To illustrate, on the 45 samples measured at 50% RH, the diameter goes from 77µm to 206 µm in a range within 1,5*IQR (inter-quartile range) before the tensile test.

Moreover, it is difficult to observe the impact of RH on the potential swelling of the samples. The main reason for this is that in the RH ranges tested, it was shown that the cross-sectional swelling was only about 10% between 20% RH and 73% RH [17]. However, this swelling may be difficult to observe if batches of different fibers are compared as opposed to monitoring the same sample under different RH. Furthermore, these data highlight that the transverse dimensions of the samples were not modified after mechanical testing.

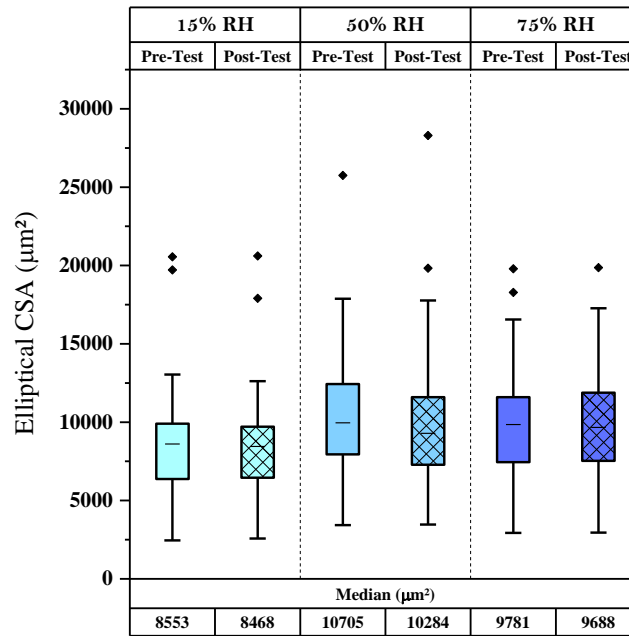


Figure 1: Boxplot of the elliptical CSA before and after tensile test of all flax bundles used in this work in function of the relative humidity.

2.4 Tensile tests

The tensile tests were carried using a micro-tensile system LEX820 (Diastron Ltd, Hampshire, UK). The initial length of the samples was fixed at ~30 mm. Each sample was subjected to 10 consecutive loading-unloading cycles. Before each cycle, the crosshead was driven up to a slight 0.02 N pre-load. The corresponding sample length measured by the apparatus was used as sample gauge length for the next loading-unloading cycle. Based on this specific and evolving gauge length over the successive cycles, the maximum strain was set at 1% for all loading cycles. This value of 1% strain at each cycle was chosen based on monotonic tensile test measurements which showed that these flax bundles had a strain at break of between 2 and 3% [10]. The objective was to observe the beginning stress-strain curve with potential non-linearity without causing breakage during all ten tensile cycles. After this loading phase, the sample undergoes an unloading phase at the same speed until it reaches the initial position of the crosshead in the first cycle. This unloading phase can therefore imply a slight buckling of the sample. Once the unloading phase is over, a new cycle starts without relaxation time. The initial gauge length used to calculate the strain of the sample during the test is always the gauge length measured by the apparatus after the pre-load at the first cycle. The acquisition frequency was adjusted from 1000 ms, 100 ms, 10 ms for tensile speeds of 0.1, 1 and 10 mm/min, respectively.

Once the ten loading-unloading cycles are completed, the stress/strain curves can be plotted for each cycle, the tensile stress being calculated as the force divided by the CSA of the sample. The displacement measured by the LEX is corrected assuming a constant system compliance of 0.03 mm/N. This compliance value was estimated using the French standard method NFT 25-501-2 [22] on flax fiber bundles. This value was corroborated by photomechanical measurements during tensile test in standard conditions (50 %RH and a speed of 1 mm/min). This correction implies a reduction in the deformation values.

An example of a corrected stress-strain curve is shown in Figure 2. The set of mechanical properties determined from the load-unload cycles are described in Table (1). These properties can be determined independently at each cycle, which makes it possible to study their evolution as a function of the number of cycles already done by the bundle.

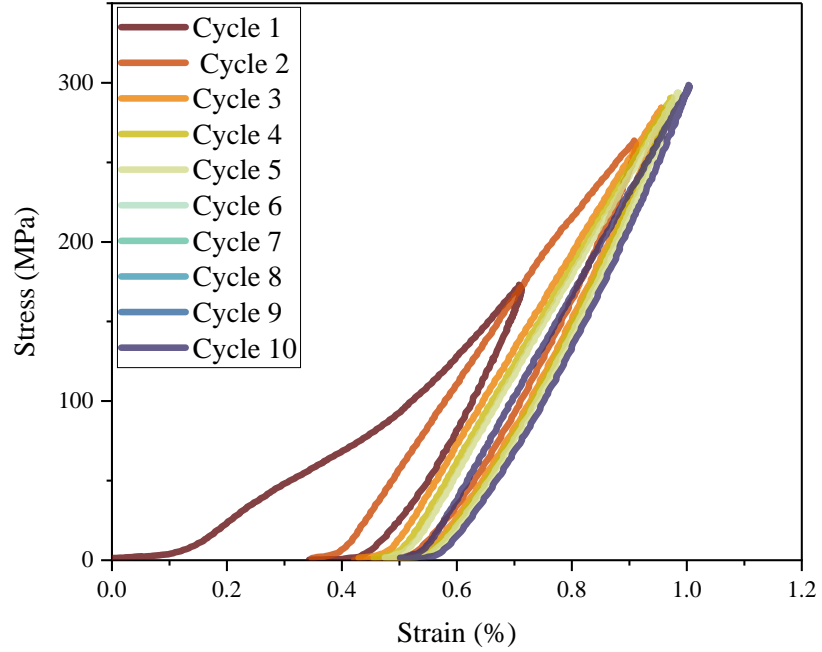


Figure 2: Stress-strain curves for a 10 load-unload cyclic tensile test on a flax bundle at 50 %RH and a tensile speed of 1 mm/min.

Properties	Designation	Definition
Initial modulus	E_{ini}	Calculated as the slope of the stress-strain curve between 0.05% and 0.5% strain
Maximum tangent modulus	E_{max}	Calculated as the maximum slope of the stress-strain curve during loading over a strain range half that used in the calculation of E_{ini}
Recovery modulus	E_{rec}	Calculated as the maximum slope of the stress-strain curve during unloading over a strain range half that used in the calculation of E_{ini}
Dissipated energy	w_h	Hysteresis dissipative energy
Residual Strain	ϵ_r	Residual deformation at the end of the unloading phase when the force reaches down 0.02N

Table 1: Main mechanical properties determined on each cyclic tensile test.

For more information, the E_{ini} is calculated as the same method used in previous work [10]. Regarding the E_{max} and E_{rec} modulus, they are calculated from slope estimation. These slopes are calculated over ranges of deformations two times smaller than that one used to calculate E_{ini} i.e. over a strain interval with an amplitude of 0.1125% on corrected strain-stress curve. During the load phase, this choice was made so that the study of these slopes could be representative of the study of potential non-linearities of the stress-strain curve. Furthermore, this choice allows E_{rec} not to consider the potential decrease in stiffness sometimes present at the end of the unloading phase. This modulus is then calculated on a part of the stress-strain curve present at the beginning of the unloading. This allows to characterize the material when his mechanical behavior is viscos-elastic without impact of the plasticity.

3 RESULTS AND DISCUSSION

3.1 Effect of load-unload cycles

In this and the next part (3.3), only data measured at 50% of relative humidity and a tensile speed of 1 mm/min are considered. This selection of 45 sample allows to discuss the impact of successive cycles without considering the potential impact of relative humidity and/or the tensile speed.

The curve presented in Figure 2 is representative of the mechanical behavior during the cyclic tests carried on all the samples. First, we observe a significant difference in the loading behavior between the first cycle and the following ones. Indeed, during this first cycle, all the tested fibers present a stiffening between the beginning and the end of the cycle. This observation can be quantified by calculating the difference between the modulus E_{ini} and E_{max} later.

To observe in more detail what happens during the first load phase it is possible to plot the evolution of the tangent modulus along the load curve. This evolution is illustrated for a selection of ten different sample in Figure 3. For all samples, as in the one presented in Figure 1, we observe a first stiffening phase at low deformation. In this first phase, the tangent modulus increases until a local maximum is reached like is illustrated in the Figure 3. This is followed by a decrease in stiffness or a constant value, illustrated in the Figure 2 like a second phase. Finally, a third phase is illustrated in Figure 3 during which the tangent modulus increases with strain.

These observations are consistent with the hypotheses described in the introduction and described by Placet et al. [11] who observed similar behavior over the same strain ranges. In other works, it is also over this same range of strain, between 0% and 1%, that the microfibrillar angle changes are observed by Placet et al. [23]. Following the charging phase, an unloading phase with a steeper slope is observed, which will be illustrated by comparing the value of E_{rec} with the other tangent modulus.

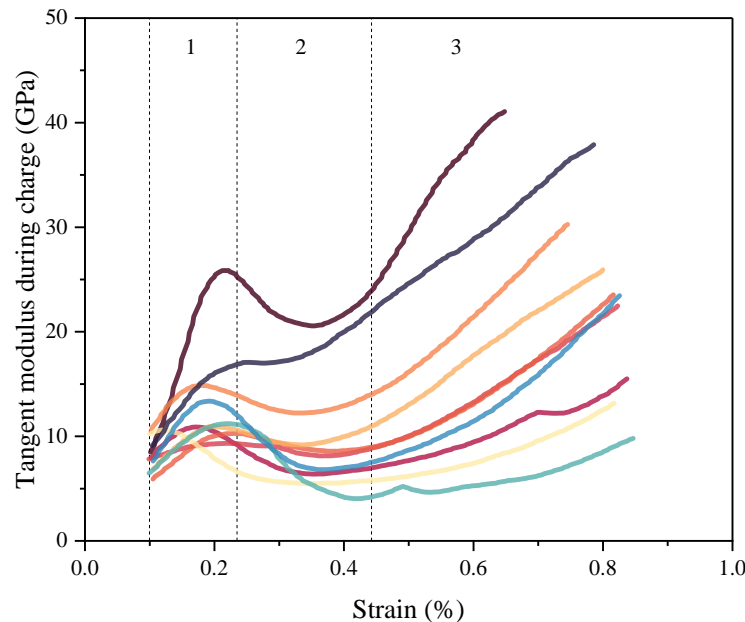


Figure 3: Tangent modulus evolution during the loading phase of the first cycle for ten different flax bundle at 1 mm/min and 50% HR.

As far as the shape of the stress-strain curve is concerned, the transition from the first cycle to the second leads to important changes: (1) a loading phase which becomes linear (2) a slope value which is strongly increasing (3) a much lower residual strain at the end of the cycle.

In all the tests, the stress-strain curves are greatly modified during the first three cycles and then hardly move after the third cycle. Therefore, to illustrate this phenomenon, the evolution of the quantities described in Table 1 will be presented between cycles 1, 2, 3 and 10.

More specifically on the modulus, Figure 4(a) illustrates the impact of the number of cycles on the

values of the modulus E_{ini} , E_{max} , E_{rec} . It can be seen that E_{ini} is strongly impacted between the first and the second cycle which agrees with the suppression of the stiffness loss phase present in the first cycle. Indeed, in the introduction, possible origins of the non-linearity of the stress-strain curve are discussed. Modification of the MFA, dislocation of certain defects or crystallization of part of the fiber structure. In the case of load-unload tests, these phenomena appear to be partly irreversible. This irreversibility could then explain why after the first cycle, the stress-strain curve no longer shows the non-linearity resulting from these different phenomena.

In a second step, once the first cycle is over, we observe that the E_{ini} and E_{max} modulus increase little by little with the number of cycles. These results are consistent with the literature which shows that the modulus increases non-linearly with deformation during the loading [12], [24].

Moreover, it is possible to observe how the evolution of the tangent modulus during the load is impacted by the number of cycles. A representative example of the full set of results is shown in Figure 4(b). For all the cycles, a phase of significant increase in the tangent modulus at very low strain is always visible. On the other hand, contrary to the first cycle, the tangent modulus evolves only slightly or not at all after this phase of rigidification. In addition, it is clearly observable that the modulus reached during this linear phase is increased between the first and the second cycle then between the second and the third cycle but hardly increases any more between cycle 3 and cycle 10.

Regarding the evolution of w_h or ε_r according to the number of cycles, this is discussed in the following part integrating the impact of the tensile speed.

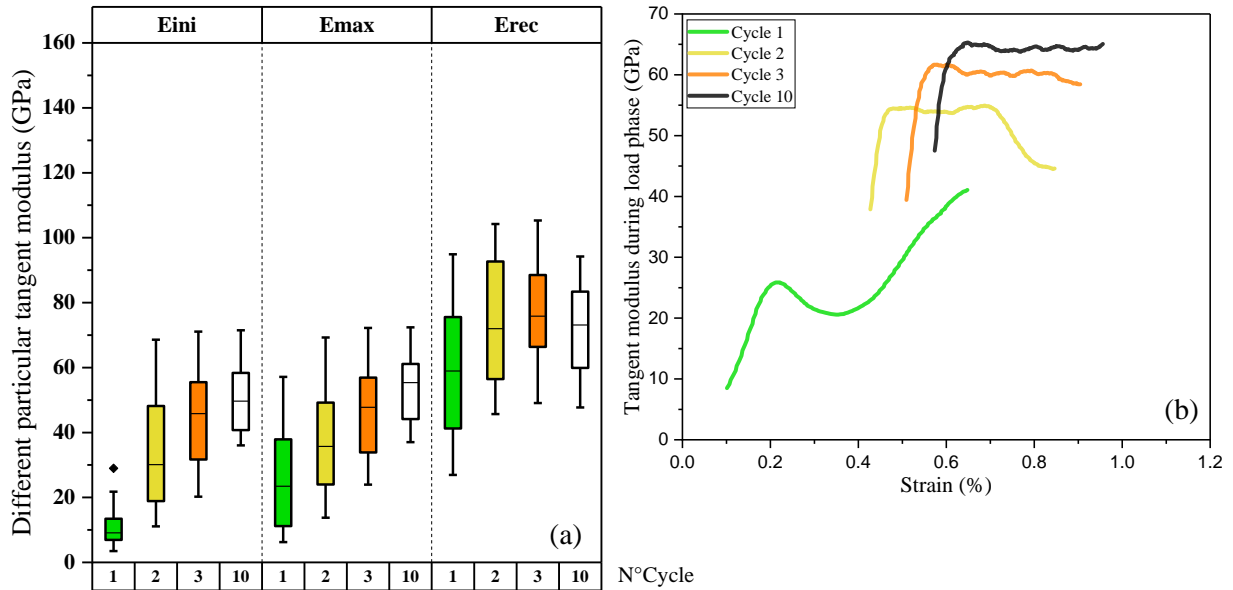


Figure 4: (a) Boxplot of E_{ini} , E_{max} and E_{rec} in function of the cycle during load-unload tensile test and (b) a representative case of the evolution of the tangent modulus during the loading phase.

3.2 Influence of the tensile speed

Regarding the different tangent modulus, it is first observed that the tensile speed does not have an impact during the loading phase. As it is represented in Figure 5(a), the values of E_{max} are similar for a specific cycle. Furthermore, the increase in E_{max} modulus as a function of the number of cycles also appears to be unaffected by speed.

However, as regards the E_{rec} measured at the beginning of the unloading, it is observed in the Figure 5(b) that it increases significantly with the tensile speed, especially at 10mm/min. This highlights the significant influence of the viscous component to the mechanical behavior of flax bundles.

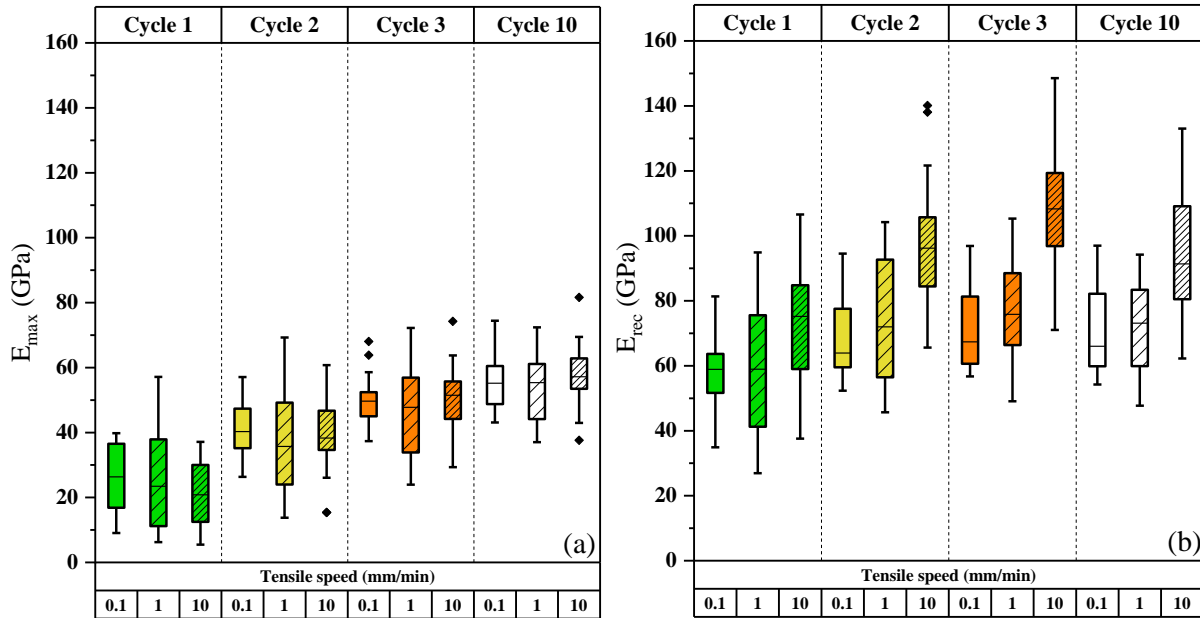


Figure 5: Boxplot of (a) E_{max} and (b) E_{rec} in function of the cycle and the tensile speed at 50 %RH.

Subsequently, regarding residual strain (ϵ_r) in the Figure 6(a), it is important to first highlight the impact of the number of cycles on this residual deformation at the end of a cycle. As can be seen in Figure 2, ϵ_r increases greatly between the first and second cycle and then stabilizes. This residual deformation highlights a potentially irreversible phenomenon.

Regarding hysteresis dissipative energy (w_h) in the Figure 6(b), this one does not seem to be impacted by the loading or unloading speed too. On the other hand, the impact of the number of cycles is interesting to highlight. Indeed, as illustrated in Figure 2, the value of w_h is important during the first cycle. But, during the second cycle, even though the hysteresis changes its shape entirely, the w_h value increase.

These first two cycles take place at lower stress and strain values than the following ones, which makes them difficult to compare with cycles from 3 to 10. However, if we compare cycles 3 and 10 only, we see a reduction of w_h . During these cycles, the stress and strain reached by the fiber are slightly modified but tend to stabilize. The observation of a decrease w_h while the stress-strain curves are stabilized implies that a part of the mechanical behaviour is visco-plastic. This part of visco-plasticity is added with visco-elasticity during the cyclic tensile test. Increasing the number of cycles implies a reduction in visco-plasticity which is consumed and therefore leads to a purely visco-elastic behaviour, which explains the reduction of w_h .

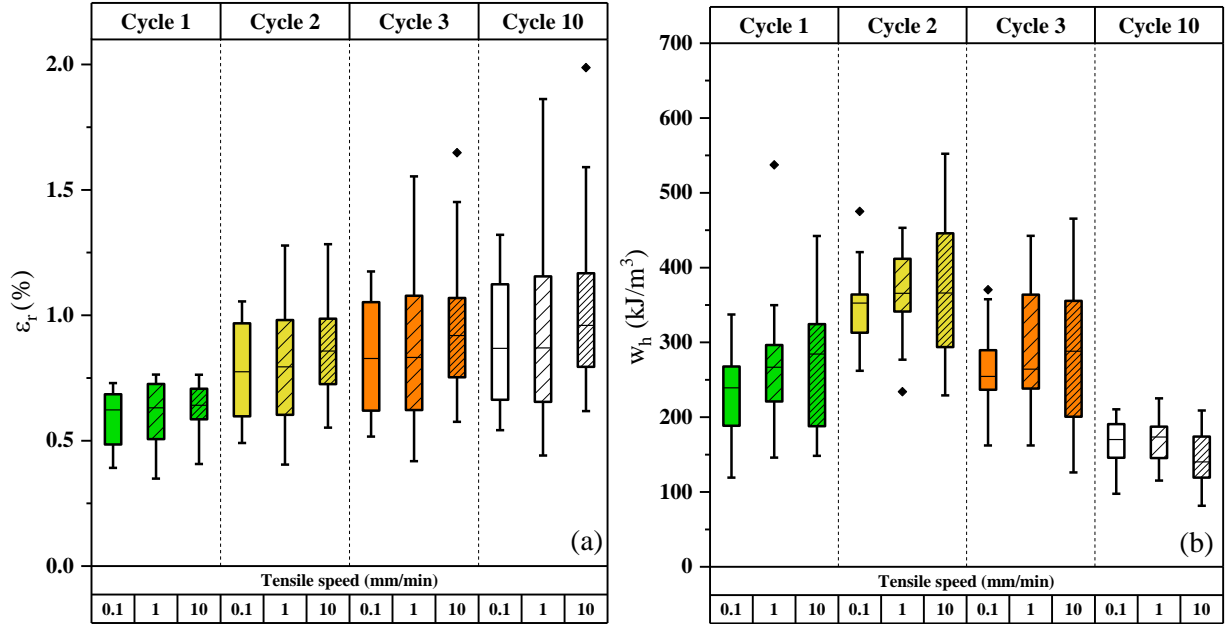


Figure 6: Boxplot of (a) ϵ_r and (b) w_h in function of the cycle and the tensile speed at 50 %RH.

3.3 Influence of the relative humidity

We observe whatever the cycle that modulus under load, i.e., the E_{ini} in Figure 7(a) and E_{max} in Figure 7(b), decrease when the relative humidity increases which is supported by existing data in literature [25], [26].

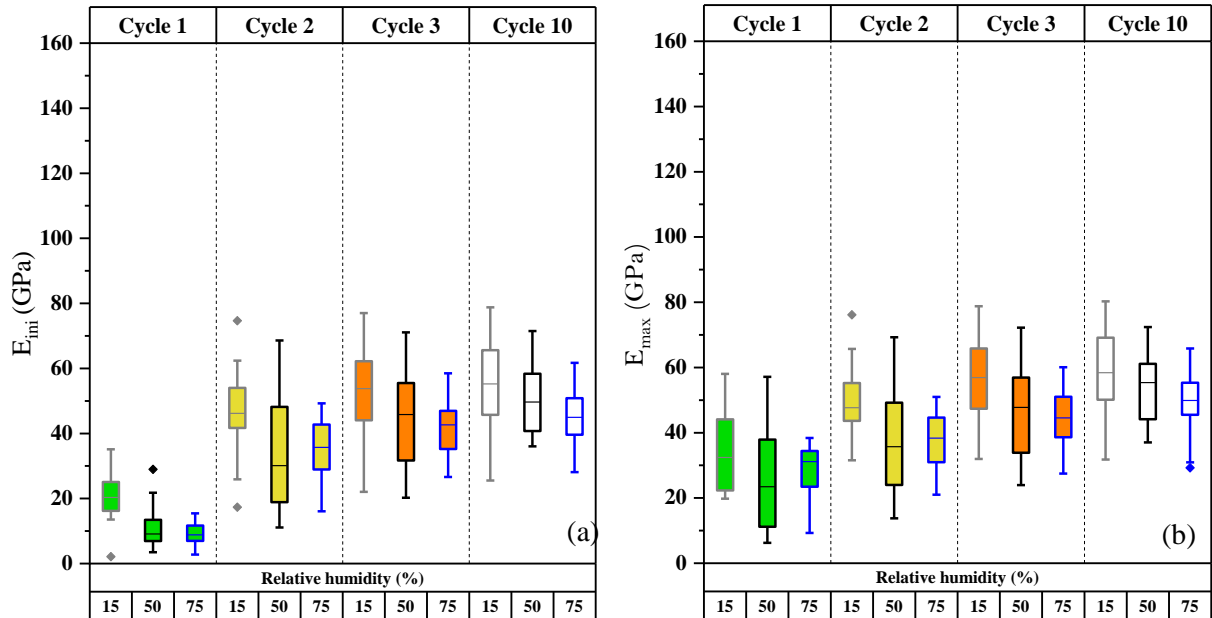


Figure 7: Boxplot of (a) E_{ini} and (b) E_{max} in function of the cycle and the relative humidity at 1mm/min.

The E_{rec} modulus also appears to decrease with increasing of RH, but less visibly than for the other tangent modulus like it is represented in Figure 8. This observation suggests that the impact of RH is limited with respect to the elastic component of the mechanical behaviour. Indeed, the E_{rec} modulus is estimated on a part of the stress-strain curve in which the viscous component of the behaviour is limited. This indicates that the RH would have an important impact on the viscous component of the mechanical behaviour, which has already been observed by creep tests on hemp fibers [14].

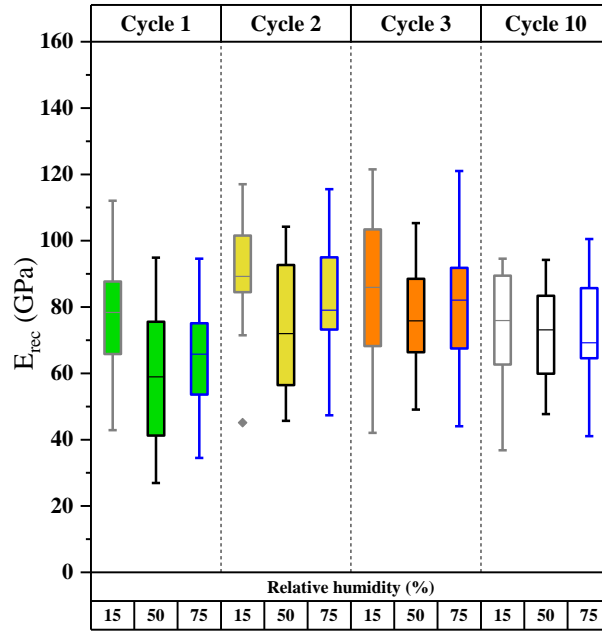


Figure 8: Boxplot of E_{rec} in function of the cycle and the relative humidity at 1mm/min.

Finally, about ϵ_r and w_h , it can be seen in the Figure 9 that it is difficult to observe an overall trend in the impact of RH over all cycles. However, it is possible to ignore the first two cycles, which take place at different stress and strain levels than cycles 3 and 10. Once the stress-strain curve has stabilized, an increase in RH implies an increase in ϵ_r and w_h . It is possible to propose the hypothesis that the increase of the moisture content in the bundles decreases the relaxation time and increases the amplitude of the deformations during the load-unload cycles. This could explain the increase in dissipated energy.

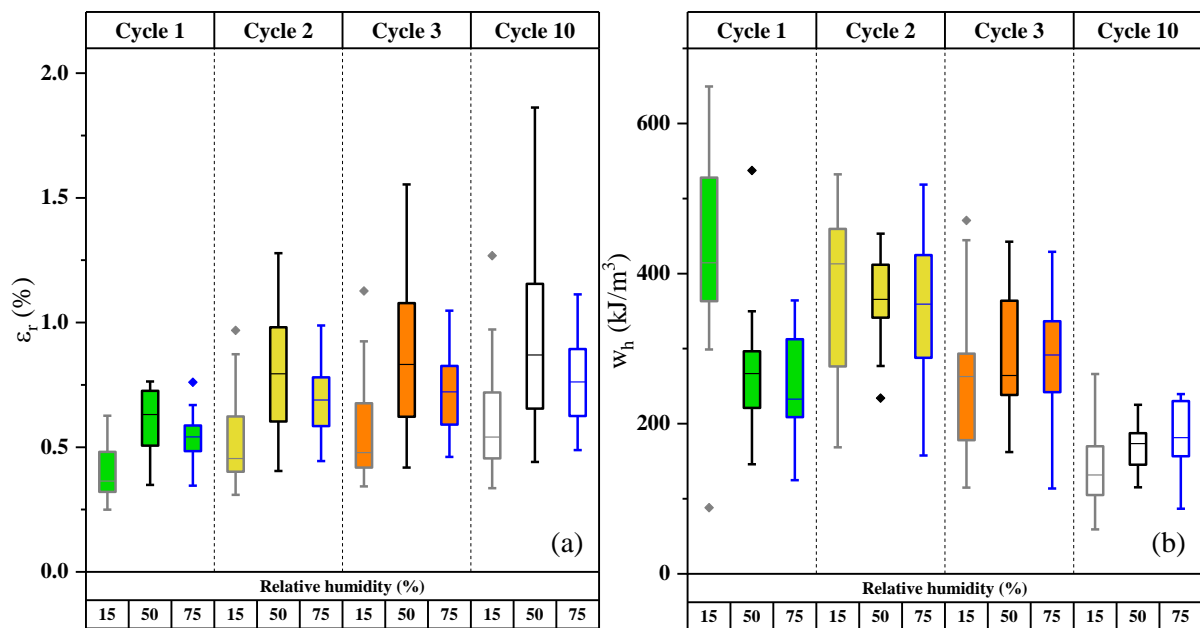


Figure 9: Boxplot of (a) ϵ_r and (b) w_h in function of the cycle and the relative humidity at 1mm/min.

4 CONCLUSIONS AND PERSPECTIVES

The visco-elasto-plastic behavior of flax fiber bundles was studied from cyclic tensile tests conducted in various conditions (crosshead speed and controlled RH). It was shown that the strong non-linearity of the mechanical response observed in the loading part of the first cycles is absent beyond the third cycle. It is hypothesized that the phenomena that may cause this non-linearity occur irreversibly during the first load cycles i.e. modification of the MFA, dislocation of certain defects or crystallization of part of the fiber structure.

As a first step, the impacts of the tensile speed on the mechanical behavior was studied. It was shown that the speed ranging from 0.1 to 10 mm/min has little influence on the mechanical properties measured during the load phase i.e. E_{ini} and E_{max} . The proposed hypothesis is that the viscous component of the behaviour is difficult to observe in a loading phase where the plastic component of the behaviour is important. In contrast, during the unloading phase, the E_{rec} modulus gives higher values when the speed is at 10 mm/min. The plasticity not being considered during this phase of unloading, the sensitivity of the modulus with the speed confirms the existence of a viscoelastic behavior.

As a second step, the impacts of the RH on the mechanical behavior was studied. First of all, it was shown that an increase of the RH implies a decrease of the E_{ini} and E_{max} during the load phase for a same speed. This shows that an increase in relative humidity tends to soften the flax bundles by affecting the visco-elasto-plastic behavior. During unloading phase, the E_{rec} modulus seems to be less affected by the increase in RH for the same speed. The proposed hypothesis is that the RH have an impact on the plasticity part of the behaviour which is visible during the load phase and not during the unload phase. This hypothesis can be combined with the hypothesis that the RH have an impact on the relaxation time of the fibre. For example, with a higher RH the relaxation time can decrease. In this case, at this speed the viscous part of the behaviour cannot be seen on E_{rec} . So, maybe, during the unloading phase, we only see the elastic part of the behaviour which can be not really impacted by the RH.

As a follow-up to this work, the study of the coupled impact of the tensile speed and the RH would make it possible to observe the impact of the RH on the viscous component of the behaviour. Moreover, further tests at the elementary flax fiber scale can be realized to analyze structural and scaling effects on mechanical behavior.

Thereafter, this research work aims to develop a mechanical model that would consider the tensile speed and RH dependence of the different components of the visco-elasto-plastic behaviour of flax bundles.

ACKNOWLEDGEMENTS

Thanks are given to the Occitanie Pyrénées-Méditerranée FRANCE region which allowed the financing of Erwan HUGUET's thesis during which this work was done.

REFERENCES

- [1] A. Bourmaud, J. Beaugrand, D. U. Shah, V. Placet, and C. Baley, "Towards the design of high-performance plant fibre composites," *Prog. Mater. Sci.*, vol. 97, no. July 2017, pp. 347–408, 2018, doi: 10.1016/j.pmatsci.2018.05.005.
- [2] C. Baley, M. Gomina, J. Breard, A. Bourmaud, and P. Davies, "Variability of mechanical properties of flax fibres for composite reinforcement. A review," *Ind. Crops Prod.*, vol. 145, p. 111984, Mar. 2020, doi: 10.1016/J.INDCROP.2019.111984.
- [3] P. R. Hornsby, E. Hinrichsen, and K. Tarverdi, "Preparation and properties of polypropylene composites reinforced with wheat and flax straw fibres: Part I Fibre characterization," *J. Mater. Sci.*, vol. 32, no. 2, 1997, doi: 10.1023/A:1018521920738.
- [4] A. Duval, A. Bourmaud, L. Augier, and C. Baley, "Influence of the sampling area of the stem on the mechanical properties of hemp fibers," *Mater. Lett.*, vol. 65, no. 4, pp. 797–800, Feb. 2011, doi: 10.1016/J.MATLET.2010.11.053.
- [5] V. Placet, "Characterization of the thermo-mechanical behaviour of Hemp fibres intended for the manufacturing of high performance composites," *Compos. - Part A Appl. Sci. Manuf.*, vol.

- 40, pp. 1111–1118, 2009.
- [6] A. Bourmaud, C. Morvan, A. Bouali, V. Placet, P. Perré, and C. Baley, “Relationships between micro-fibrillar angle, mechanical properties and biochemical composition of flax fibers,” *Ind. Crops Prod.*, vol. 44, pp. 343–351, Jan. 2013, doi: 10.1016/J.INDCROP.2012.11.031.
- [7] M. Sedighi Gilani, “A micromechanical approach to the behaviour of single wood fibers and wood fracture at cellular level,” 2006, doi: 10.5075/EPFL-THESIS-3546.
- [8] E. Richely, A. Bourmaud, V. Placet, S. Guessasma, and J. Beaugrand, “A critical review of the ultrastructure, mechanics and modelling of flax fibres and their defects,” *Prog. Mater. Sci.*, vol. 124, p. 100851, Feb. 2022, doi: 10.1016/J.PMATSCI.2021.100851.
- [9] O. M. Astley and A. M. Donald, “The tensile deformation of flax fibres as studied by X-ray scattering,” *J. Mater. Sci.*, vol. 38, no. 1, pp. 165–171, Jan. 2003, doi: 10.1023/A:1021186421194/METRICS.
- [10] E. Huguet, S. Corn, N. Le Moigne, and P. Jenny, “Contribution à la caractérisation du comportement mécanique de fibres végétales en environnement contrôlé : fiabilisation d’un essai de traction,” 2022.
- [11] V. Placet, O. Cissé, and M. Lamine Boubakar, “Nonlinear tensile behaviour of elementary hemp fibres. Part I: Investigation of the possible origins using repeated progressive loading with in situ microscopic observations,” *Compos. Part A Appl. Sci. Manuf.*, vol. 56, 2014, doi: 10.1016/j.compositesa.2012.11.019.
- [12] C. Baley, “Analysis of the flax fibres tensile behaviour and analysis of the tensile stiffness increase,” *Compos. - Part A Appl. Sci. Manuf.*, vol. 33, no. 7, 2002, doi: 10.1016/S1359-835X(02)00040-4.
- [13] V. Guicheret-Retel, O. Cisse, V. Placet, J. Beaugrand, M. Pernes, and • M Lamine Boubakar, “Creep behaviour of single hemp fibres. Part II: Influence of loading level, moisture content and moisture variation,” doi: 10.1007/s10853-014-8768-0.
- [14] O. Cisse, V. Placet, V. Guicheret-Retel, F. Trivaudey, and M. L. Boubakar, “Creep behaviour of single hemp fibres. Part I: viscoelastic properties and their scattering under constant climate,” *J. Mater. Sci.*, vol. 50, no. 4, pp. 1996–2006, Feb. 2015, doi: 10.1007/S10853-014-8767-1/TABLES/4.
- [15] Y. Yu, Z. Jiang, B. Fei, G. Wang, and H. Wang, “An improved microtensile technique for mechanical characterization of short plant fibers: A case study on bamboo fibers,” *J. Mater. Sci.*, vol. 46, no. 3, pp. 739–746, Feb. 2011.
- [16] V. Keryvin, M. Lan, A. Bourmaud, T. Parenteau, L. Charleux, and C. Baley, “Analysis of flax fibres viscoelastic behaviour at micro and nano scales,” *Compos. Part A Appl. Sci. Manuf.*, vol. 68, pp. 219–225, 2015, doi: 10.1016/J.COMPOSITESA.2014.10.006.
- [17] W. Garat, N. Le Moigne, S. Corn, J. Beaugrand, and A. Bergeret, “Swelling of natural fibre bundles under hygro- and hydrothermal conditions: Determination of hydric expansion coefficients by automated laser scanning,” *Compos. Part A Appl. Sci. Manuf.*, vol. 131, no. September 2019, 2020, doi: 10.1016/j.compositesa.2020.105803.
- [18] V. Placet, O. Cisse, and M. L. Boubakar, “Influence of environmental relative humidity on the tensile and rotational behaviour of hemp fibres,” *J. Mater. Sci.*, vol. 47, no. 7, 2012, doi: 10.1007/s10853-011-6191-3.
- [19] F. Dong, A. M. Olsson, and L. Salmén, “Fibre morphological effects on mechano-sorptive creep,” *Wood Sci. Technol.*, vol. 44, no. 3, 2010, doi: 10.1007/s00226-009-0300-3.
- [20] W. Garat, N. Le Moigne, J. Beaugrand, P. Jenny, and A. Bergeret, “Dimensional Variations and Mechanical Behavior of Various Plant Fibre Species under Controlled Hydro / Hydrothermal Conditions Variations Dimensionnelles et Comportement Mécanique de Plusieurs Espèces de Fibres Végétales en Conditions Hydro / Hydrothe,” *Rev. des Compos. des Matériaux Avancés*, vol. 29, no. 5, pp. 299–304, 2019.
- [21] W. Garat, S. Corn, N. Le Moigne, J. Beaugrand, and A. Bergeret, “Analysis of the

- morphometric variations in natural fibres by automated laser scanning: Towards an efficient and reliable assessment of the cross-sectional area,” *Compos. Part A Appl. Sci. Manuf.*, vol. 108, no. November 2017, pp. 114–123, May 2018, doi: 10.1016/j.compositesa.2018.02.018.
- [22] NF T25-501-2, “Fibres de renfort — Fibres de lin pour composites plastiques — Partie 2 : Détermination des propriétés en traction des fibres élémentaires,” *Norme française AFNOR*, 2015.
- [23] V. Placet, A. Bouali, C. Garcin, J.-M. Cote, P. Perré, and P. P. Suivi, “Suivi par DRX des réarrangements microstructuraux induits par sollicitations mécaniques dans les fibres végétales tirées du chanvre,” Aug. 2011, Accessed: May 10, 2023. [Online]. Available: <https://hal.science/hal-03421227>.
- [24] E. Bodros, I. Pillin, N. Montrelay, and C. Baley, “Could biopolymers reinforced by randomly scattered flax fibre be used in structural applications?,” *Compos. Sci. Technol.*, vol. 67, no. 3–4, 2007, doi: 10.1016/j.compscitech.2006.08.024.
- [25] G. C. Davies and D. M. Bruce, “Effect of Environmental Relative Humidity and Damage on the Tensile Properties of Flax and Nettle Fibers,” *Text. Res. J.*, vol. 68, no. 9, 1998, doi: 10.1177/004051759806800901.
- [26] M. C. Symington, W. M. Banks, O. D. West, and R. A. Pethrick, “Tensile testing of cellulose based natural fibers for structural composite applications,” in *Journal of Composite Materials*, 2009, vol. 43, no. 9, doi: 10.1177/0021998308097740.